DOI: 10.61782/fa.2023.1090

forum acusticum 2023

VALIDATION OF AN EIGENVALUE TECHNIQUE FOR ESTIMATING LOCALLY REACTING IMPEDANCES AT MODAL FREQUENCIES

Albert G. Prinn[1*] **Andreas Walther**[1] **Emanuël A. P. Habets**[2]

[1] Fraunhofer IIS, Erlangen, Germany
[2] International Audio Laboratories Erlangen[†], Germany

ABSTRACT

For computational room acoustics, accurate surface impedance data is needed to generate computational models that aim to provide accurate predictions. However, obtaining complex-valued frequency-dependent impedances of an acoustically absorbing material at low frequencies is a challenging task. In point of fact, the current measurement standard ISO 354:2003, which describes the measurement of absorption coefficients (which can be related to impedance) in a reverberation chamber, states that it is difficult to obtain reliable data below 100 Hz. There is therefore a need for advanced low-frequency measurement techniques. This paper presents a validation of a recently proposed eigenvalue-based inverse method for estimating locally reacting impedances at modal frequencies. The proposed method is validated using data measured in an impedance tube. This method can be used to estimate the sample impedance in reverberant rooms at low frequencies.

Keywords: *Impedance estimation, Eigenvalue analysis, Finite element method, Low frequency*.

**Corresponding author*: albert.prinn@iis.fraunhofer.de
[†]*A joint institution of the Friedrich-Alexander-Universität Erlangen-Nürnberg (FAU) and Fraunhofer IIS, Germany.*

1. INTRODUCTION

For a valid computational acoustic model to provide faithful predictions, the input parameters must be accurate (see, e.g., Refs. [1–6]). For interior acoustics simulations, accurate descriptions of source characteristics, room geometry, and room surface impedances are required. Obtaining accurate impedance descriptions of material samples at low frequencies is a challenging task, which often requires the use of dedicated setups, for example, the measurement of a sample in a specially designed impedance tube (e.g., Ref. [7]). While the impedance tube does provide accurate measurements, it is of limited use when attempting to measure the impedances of acoustically absorbing materials that are already installed in a room. In such cases, one may consider measurement in a reverberation chamber; However, this measurement method provides Sabine absorption coefficients, not complex-valued impedances, and it is not reliable at low frequencies [8] due to measurement uncertainty (see, for example, Wittstock [9]). In this paper, a method recently proposed by the current authors for estimating complex-valued impedances at modal frequencies [10] is validated using impedance tube measurements.

Various similar methods can be found in the literature. Dutilleux *et al.* [11] present a boundary inverse interior problem and apply it to the estimation of complex-valued impedances at low frequencies in a room. Use is made of the finite element and finite difference methods, and promising solutions are obtained in a set of simulated problems. Anderssohn and Marburg [12] also make use of the finite element method to estimate complex-valued admittance. Nonlinear optimization is used to obtain non-uniform, frequency-independent surface admittance esti-

mates in a simulated car cabin. Nava *et al.* [13] present an inverse method based on the boundary element method. They estimate the complex impedance of samples placed in a small chamber. The method is validated by showing that the error between the measured and simulated pressure fields is small. Bockman *et al.* [14] present a Bayesian impedance estimation method. The method is validated using impedance tube measurements.

An eigenvalue-based impedance estimation method is given by Hull and Radcliffe [15]. They estimate the impedance of a sample of foam in an impedance tube using an analytical description of the eigenvalues of a rigid-walled impedance tube terminated by an absorbing surface. Good results are found with measured data. More recently, Nowakowski *et al.* [16] estimate impedance using the measured eigenmodes of a system under test. Good results are obtained for a simulated, two-dimensional problem. For the interested reader, an informative review of in-situ impedance measurement methods is given by Brandão *et al.* [17].

All the methods described above (except for Hull and Radcliffe [15]) make use of optimization to obtain impedance estimates; This is because these works estimate non-uniform impedances. While the method considered here can be combined with an optimization routine, as shown by Prinn *et al.* [10], in this work, a uniform sample impedance is estimated, with the result that optimization is not needed. As input data, the method requires knowledge of the geometry of the system under test and an impulse response measured at a single position. In this work, the finite element method is used to assemble the system matrices, which are then used to estimate the impedance of a sample in an impedance tube.

The remainder of this paper is organized as follows. In Sec. 2, an overview of the proposed impedance estimation method is presented. In Sec. 3, the measurement setup and estimates of the complex-valued impedance of a sample are presented. The method is further discussed in Sec. 4, and the paper is concluded in Sec. 5.

2. IMPEDANCE ESTIMATION METHOD

The proposed impedance estimation method [10] is briefly reviewed in this section. The method comprises two parts: (1) complex-valued eigenvalues that identify the modal frequencies and modal damping coefficients of the system under test are measured or estimated, and (2) an inverse eigenvalue-based problem of the system is solved to provide estimates of a sample's locally reacting impedance.

2.1 Eigenvalue estimation

In this work, the eigenvalues are estimated using the approach described by Prinn et al. [18]. For conciseness, the approach is only briefly described here. The eigenvalues are estimated using the matrix pencil method [19]. This method accepts an impulse response and generates and solves an eigenvalue problem. A set of candidates for the eigenvalue estimates, $\hat{\lambda}$, is then available. However, although the matrix pencil method provides good estimates, it also provides a significant number of spurious solutions (see, e.g., Refs. [18, 20, 21]). The spurious solutions must be identified and removed if one is to obtain a set of valid solutions. The approach used in this work to remove the spurious solutions is described in Sec. 3.2.2.

2.2 Impedance estimator

To estimate the impedance, two eigenvalue systems are constructed: a first that models the measurement system with known impedance, and a second that models the system with an unknown sample impedance. If the eigenmodes of a given system are weakly coupled, an eigenvalue of the second system can be approximated using the formula

$$\hat{\lambda}_j^{(1)} = \lambda_j^{(0)} \frac{\left(\boldsymbol{v}_j^{(0)}\right)^{\mathrm{T}} \left(\mathbf{C}^{(0)} + 2\lambda_j^{(0)}\mathbf{M}\right) \boldsymbol{v}_j^{(0)}}{\left(\boldsymbol{v}_j^{(0)}\right)^{\mathrm{T}} \left(\mathbf{C}^{(1)} + 2\lambda_j^{(0)}\mathbf{M}\right) \boldsymbol{v}_j^{(0)}}, \qquad (1)$$

where $\mathbf{C}$, and $\mathbf{M}$ are damping and mass matrices, λ_j and $\boldsymbol{v}_j$ are the jth eigenvalue and eigenvector, and superscripts (0) and (1) identify the first and second system, respectively. A full derivation of Eq. (1) can be found in the article by Prinn *et al.* [10]. Note that the damping matrix includes a c^{-1} term, and the mass matrix includes a c^{-2} term, where c is the speed of sound. The subscript j is omitted for brevity from this point onward (except where needed).

We proceed by writing the damping matrix of the second system as

$$\mathbf{C}^{(1)} = \zeta_s^{-1}\mathbf{C}_s^{(1)} + \zeta_w^{-1}\mathbf{C}_w^{(1)} + \zeta_z^{-1}\mathbf{C}_z^{(1)}, \qquad (2)$$

where subscript s represents a source's surface, subscript w represents a wall's surface, and subscript z represents an impedance sample's surface. Assuming the estimated eigenvalues $\hat{\lambda}$ (cf. Sec. 2.1) are valid estimates of $\hat{\lambda}^{(1)}$, Eq. (1) can be rewritten to give an estimate for an unknown impedance at the jth mode. For example, when

the impedances at the source and wall are known, the sample's impedance is approximated by

$$\hat{\zeta}_z = \frac{\hat{\lambda}^{(1)} \left(\boldsymbol{v}^{(0)}\right)^{\mathrm{T}} \mathbf{C}_z^{(1)} \boldsymbol{v}^{(0)}}{\lambda^{(0)} \left(\boldsymbol{v}^{(0)}\right)^{\mathrm{T}} S_0 \boldsymbol{v}^{(0)} - \hat{\lambda}^{(1)} \left(\boldsymbol{v}^{(0)}\right)^{\mathrm{T}} S_1 \boldsymbol{v}^{(0)}} , \quad (3)$$

where

$$\begin{aligned} S_0 &= \mathbf{C}^{(0)} + 2\lambda^{(0)}\mathbf{M} \text{ , and ,} \\ S_1 &= \zeta_s^{-1}\mathbf{C}_s^{(1)} + \zeta_w^{-1}\mathbf{C}_w^{(1)} + 2\lambda^{(0)}\mathbf{M} . \end{aligned} \quad (4)$$

Noting that Eq. (1) provides only approximate eigenvalues, the impedance estimates obtained can be used to iteratively refine the estimates given by Eq. (3), i.e., the impedance estimates from a previous iteration step are used to generate new eigensolutions, $\lambda_j^{(0)}$ and $\boldsymbol{v}_j^{(0)}$, for the current iteration step. To reduce computational effort, Rayleigh quotient iteration can be used to generate the new reference eigensolutions. For conciseness, this approach is not described here – for a detailed description of the iterative approach, see Prinn [22].

The geometries considered in this work are discretized using tetrahedral meshes, which are generated by Gmsh [23]. The finite element method is used to generate the damping and mass matrices. Quadratic interpolating functions are used, with a nodal spacing that ensures 10 degrees of freedom per wavelength at the highest frequency of interest. Note that the impedance estimation method does not require the use of the finite element method - any method capable of generating stiffness, damping, and mass matrices may be used.

3. IMPEDANCE TUBE

An impedance tube was used to measure the complex-valued impedance of a material sample. In this section, the measurement is described, and the measured and estimated impedances are compared.

3.1 Measurement setup

An impedance tube with length $L = 1.038$ m and diameter $d = 0.1$ m was used. A schematic of the impedance tube is shown in Fig. 1. The measurements were performed according to the measurement standard ISO 10534-2 [24]. For the measurements, three microphones were placed inside the tube. However, for the impedance estimations presented in what follows, only one microphone is used. The position of the microphone used for the estimations is indicated in Fig. 1.

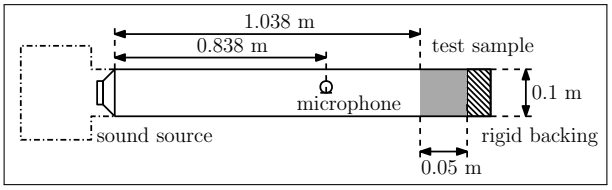

Figure 1. Schematic of the impedance tube (not to scale). The dashed lines indicate a sound insulating box with undefined dimensions, and unknown impedance.

Two impulse responses were measured in the tube. The first is that of the empty tube, the other measurement was made with the test sample installed in the tube. The measured impulse responses are shown in Fig. 2. Longer impulse responses were measured, but for the eigenvalue estimation the impulse responses are truncated to reduce the computational effort.

The sample is a foam made of melamine resin. It has a cylindrical height of 50 mm, and a weight of 3.7 g. The measured complex-valued impedance and absorption coefficients of the sample are presented in Sec. 3.2.4.

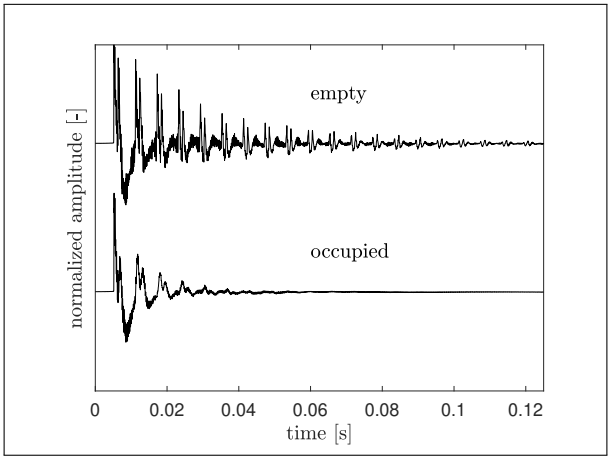

Figure 2. Measured impulse responses of the empty and occupied impedance tube.

3.2 Estimates

In this section, the estimates computed from the measured impulse responses are presented. Estimates of the speed of sound, the system eigenvalues, and the impedances of the empty tube and the occupied tube are presented.

3.2.1 *Speed of sound estimation*

The speed of sound was not recorded at the time of the measurement. Instead, it was estimated from the impulse response measured in the empty tube. First, the arrival times of the direct sound and the first four reflections are determined. The average travel time between the peaks, $\langle t \rangle$, is then used to estimate the speed of sound: $c = 2L/\langle t \rangle$. Using this procedure, we estimate that the speed of sound is $c = 344$ m/s. This value is used in the remainder of this work.

3.2.2 *Eigenvalue estimates*

Due to the simplicity of the impedance tube problem (i.e., planes waves traveling along a cylindrical duct, and thus clearly separated peaks in the transfer function), the following approach is adopted for estimating the eigenvalues:

1. peak finding is performed on the transfer function (given by Fourier transform of the impulse response) to identify candidate modal frequencies,
2. the modal frequencies of a rigid walled version of the impedance tube (idealized as a cylindrical duct) are computed analytically, and used to refine the set of candidate modal frequencies,
3. for each candidate modal frequency, f, a related damping coefficient, σ, is computed, using the short-time Fourier transform and the approach presented by Karjalainen *et al.* [25],
4. the estimated modal frequencies and damping coefficients are combined to give a set of initial estimates for the eigenvalues, $\lambda_0 = \mathrm{i}(2\pi f + \mathrm{i}\sigma)$, and
5. the matrix pencil is constructed, and the initial guesses are used to perform Rayleigh quotient iteration to find a set of candidate eigenvalues, $\hat{\lambda}$, following Ref. [18].

The estimated eigenvalues are presented, in terms of modal frequencies and damping coefficients, in Fig. 3. Estimates are given for both the empty and occupied conditions of the tube. The empty tube does not have rigid walls; This can be inferred from the significant decay of its impulse response (see Fig. 2) and is further evidenced by the non-zero damping coefficients (Fig. 3). It is assumed that this damping is located at the source side of the tube, and thus that the duct wall and rigid backing have high impedances. The rigid walled modal frequencies are compared to the estimated modal frequencies of the empty tube in Tab. 1. There is a notable change in modal frequency. For example, the fundamental frequency of the rigid walled tube is 165.7 Hz, while the fundamental frequency of the empty tube is 174.58 Hz. In general, the sample in the tube causes significant changes to the modal frequencies and damping coefficients. In the next section, we use the estimated eigenvalues to estimate the complex-valued impedances of the source side of the empty tube.

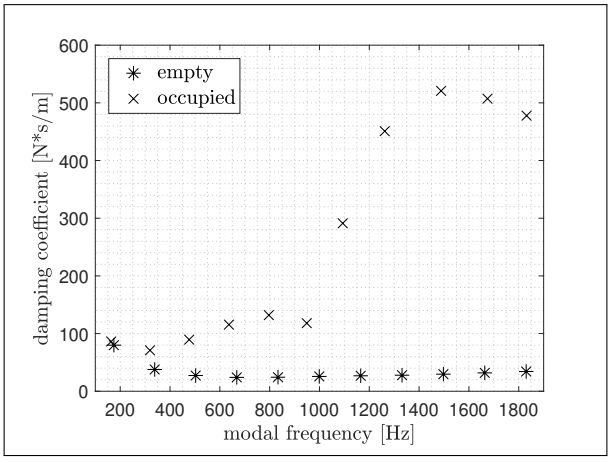

Figure 3. Estimated modal frequencies and damping coefficients of the empty tube, and the occupied tube.

Table 1. Comparison of computed rigid walled tube modal frequencies, and estimated empty tube modal frequencies.

mode number	rigid tube	empty tube
1	165.70	174.58
2	331.41	338.44
3	497.11	502.95
4	662.81	667.99
5	828.52	833.53
6	994.22	999.18
7	1159.92	1165.55
8	1325.63	1331.47
9	1491.33	1497.52
10	1657.03	1663.68
11	1822.74	1829.95

3.2.3 Empty tube estimates

It can be concluded from Fig. 3 that the modal damping coefficients of the empty tube are not negligible. This is expected, and is caused by the sound insulating box that surrounds the speaker [26, Fig. 4]. Therefore, before we can estimate the impedances of the sample, $\hat{\zeta}_z$, we must first estimate the impedance of the empty tube. It is assumed, due to the consideration of a frequency range that permits only plane waves, that the wall of the tube has an infinitely high impedance, $\zeta_w = \infty$. It is further assumed that the rigid backing at the sample end of the tube has a normalized impedance of $\zeta_z = 1 \times 10^3$, based on the following reasoning: the rigid backing should be acoustically hard, but is unlikely to have infinite impedance, and for $\zeta_z \gtrapprox \times 10^3$ the error levels of the impedance estimates (presented in Sec. 3.2.4) do not change significantly. The impedance at the source end of the tube is now estimated, by solving Eq. (3) for $\hat{\zeta}_s$.

For the impedance estimations in the impedance tube, ten iterations of the estimation are performed. For the first iteration, the analytical solutions of the rigid duct are used: $\lambda_j^{(ap)} = \mathrm{i}c\pi j/L$ and $\boldsymbol{v}_j^{(ap)} = \cos(j\pi x/L)$. Impedance estimates from the tenth iteration are shown in Fig. 4. The real part of the estimated impedance is small, and the imaginary part is positive. It is this positive imaginary part that causes the modal frequencies to shift upwards, when compared to the modal frequencies of the rigid tube (cf. Tab. 1). Shown in Fig. 5 are the corresponding absorption coefficients. There is significant damping at the fundamental frequency and non-negligible damping in general.

These estimates are used to define the impedance at the source side of the empty tube, i.e., $\zeta_s = \hat{\zeta}_s$, which are in turn used to estimate the impedances of the sample in the next section. Note that the analytical method described by Hull and Radcliffe [15] provides impedance estimates of the empty tube that agree agree with those presented in this section, with a relative error of 0.84 %. However, the analytical method assumes that one end of the impedance tube is totally reflective, and therefore, for the problem considered here, the analytical method fails to accurately estimate the impedances of the sample. Additionally, the analytical approach cannot be used for more general measurement system geometries, e.g., a reverberation chamber.

3.2.4 Sample impedance estimates

For each estimated modal frequency, the complex-valued impedance is estimated by solving Eq. (3). At each of ten iterations, the reference system is updated with the current impedance estimate. The error of the estimated impedance is computed using the formula

$$\eta_j = 100\,\frac{|\zeta_z(f_j) - \hat{\zeta}_z(f_j)|}{|\zeta_z(f_j)|}\,, \tag{5}$$

where f_j is the jth modal frequency. Cubic interpolation is used to find the corresponding data points, $\zeta_z(f_j)$, from the measured data. The error incurred while estimating the impedance for the sample is shown as a function of iteration number in Tab. 2.

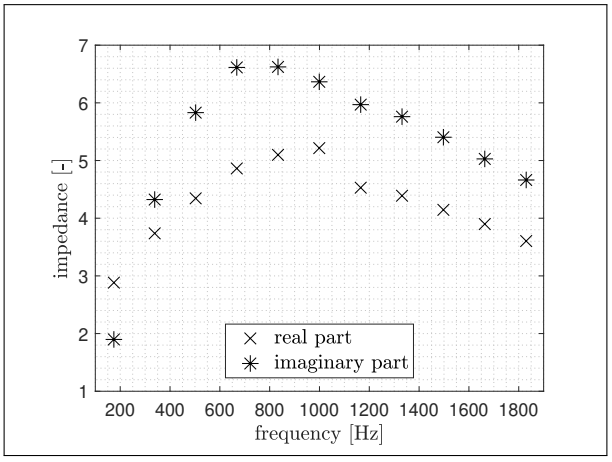

Figure 4. Estimated impedance of the source side of the empty tube. This data is used to estimate the sample impedance.

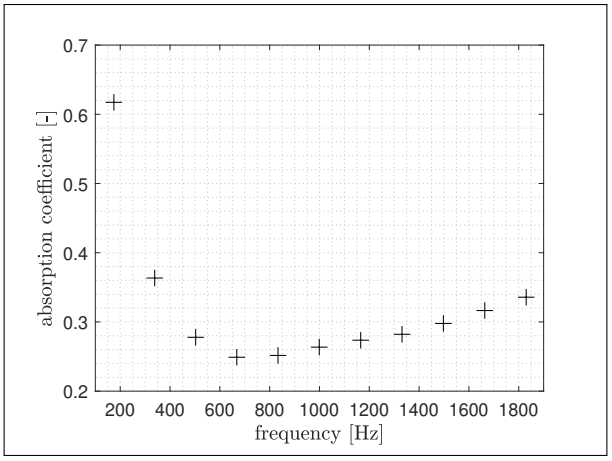

Figure 5. Absorption coefficient of the estimated empty tube impedance, shown in Fig. 4

Table 2. Impedance estimation error (in %) as a function of iteration number (it.).

modal frequency [Hz]	it. 1	it. 2	it. 3	it. 4	it. 5	it. 6	it. 7	it. 8	it. 9	it. 10
163.70	19.62	7.17	7.20	7.20	7.20	7.20	7.20	7.20	7.20	7.20
319.44	209.10	58.43	1.29	0.77	0.77	0.77	0.77	0.77	0.77	0.77
476.91	59.11	4.09	3.36	3.36	3.36	3.36	3.36	3.36	3.36	3.36
636.43	29.61	2.97	3.06	3.06	3.06	3.06	3.06	3.06	3.06	3.06
796.79	24.97	4.57	4.03	4.03	4.03	4.03	4.03	4.03	4.03	4.03
948.92	34.19	15.85	14.45	14.44	14.44	14.44	14.44	14.44	14.44	14.44
1093.40	42.98	32.20	14.21	9.66	9.97	9.97	9.97	9.97	9.97	9.97
1262.03	38.35	53.41	9.65	8.05	7.33	7.39	7.39	7.39	7.39	7.39
1488.30	9.32	7.75	6.85	6.85	6.85	6.85	6.85	6.85	6.85	6.85
1674.57	19.66	3.07	1.81	1.71	1.71	1.71	1.71	1.71	1.71	1.71
1831.59	12.09	6.10	7.18	7.14	7.14	7.14	7.14	7.14	7.14	7.14

We observe that the error remains constant after five iterations. Impedance estimations (tenth iteration) for the sample are compared to measured impedances in Fig. 6. The impedance at the lowest modal frequency is poorly estimated. It may be that the eigenvalue estimations (given by the matrix pencil method) are not accurate enough, or that the impedance estimate of the empty tube is not accurate enough to accurately estimate this impedance. Aside from this data point, the estimates tend to agree with the measured data. An interesting phenomenon can be seen in the estimates; Below approximately 1.5 kHz the modal frequencies are shifted downwards, compared to the rigid walled frequencies, while above 1.5 kHz the modal frequencies are shifted upwards. This is caused by the imaginary part of the impedance going from negative to positive; It is a demonstration of the sample's reactance. Shown in Fig. 7 is a comparison of the measured and estimated absorption coefficients. Good agreement is found.

While the estimates agree with the measured data, the proposed method is no substitute for the impedance tube measurement method in this frequency range. This is due to the limitation that estimations can only be performed at modal frequencies. However, the proposed method enables estimates of complex-valued impedance below 100 Hz in reverberant spaces, which means impedance estimates can be obtained without specialized impedance tubes.

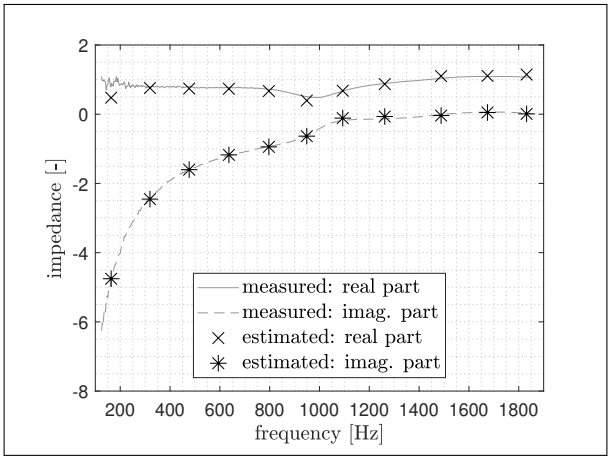

Figure 6. The measured and estimated impedance of the sample, as a function of frequency.

4. DISCUSSION

While the results demonstrate that the proposed method provides reasonable estimates of complex-valued impedances, it does so only at modal frequencies. However, for some applications, the proposed method has a significant advantage, for example, when attempting to measure complex impedance at low frequencies in a reverberation chamber. If the impedance curve is smooth enough, one might consider using polynomial or spline fitting to generate continuous frequency data. Note, as

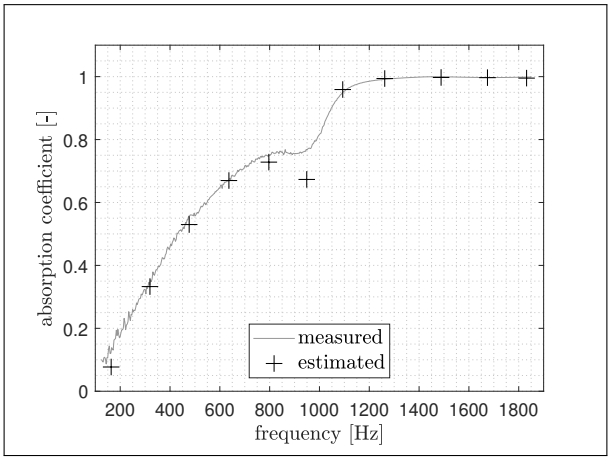

Figure 7. Measured and estimated absorption coefficient data for the sample, as a function of frequency.

demonstrated by Prinn *et al.* [10], the size of the sample does not appear to influence the impedance estimation. Future work should consider using the method to measure complex-valued impedance in a reverberation chamber.

Other applications of the proposed method can be envisioned. For audio applications, for example, it can be beneficial to know the impedances of the surfaces of a listening space. This is because reliable impedance information, along with geometry and source descriptions, allows one to model the sound field throughout the listening space. In such cases, it might be sufficient to have impedance estimates at the modal frequencies only, because the Q-factors of the transfer function peaks are determined by the impedance at modal frequencies, and for a given room the eigenvalues are not expected to change significantly with slight changes to the listening environment. Furthermore, this work demonstrates that the proposed method can estimate the impedance of highly damped surfaces. In common listening environments (for example, living rooms) the absorption coefficients of the acoustically absorbing surfaces are typically low, which implies surfaces that are not highly damped. Thus, it is expected that the proposed method could be used to adequately estimate impedances in common listening environments.

One additional aspect that would need to be considered is the solution of spaces with non-uniform surface impedances. For those types of problems, global optimization routines might be used to provide useful estimates. Alternatively, one might choose to estimate an average impedance for all surfaces in a room.

5. CONCLUSION

A method based on eigenvalue approximation that estimates complex-valued, frequency-dependent, locally-reacting surface impedance at modal frequencies has been validated using data measured in an impedance tube.

Future studies should consider the estimates of the complex-valued impedances of samples measured in reverberation chambers. Additionally, problems with non-uniform surface impedance might be tackled using a global optimization routine. Finally, this method could be improved by using an eigenvalue estimation method that is more robust to noise than the matrix pencil method.

6. ACKNOWLEDGMENTS

The authors would like to thank Dr. Moritz Späh and his team at Fraunhofer IBP for the impedance tube data.

7. REFERENCES

[1] M. Aretz and J. Knutzen, "Uncertainty in acoustic boundary characterisation and its influence on the sound field in room acoustic FE simulations," *Proc. DAGA, Rotterdam*, 2009.

[2] M. Vorländer, "Computer simulations in room acoustics: Concepts and uncertainties," *J. Acoust. Soc. Am.*, vol. 133, no. 3, pp. 1203–1213, 2013.

[3] M. Aretz and M. Vorländer, "Combined wave and ray based room acoustic simulations of audio systems in car passenger compartments, Part II: Comparison of simulations and measurements," *Appl. Acoust.*, vol. 76, pp. 52–65, 2014.

[4] C.-H. Jeong, G. Marbjerg, and J. Brunskog, "Uncertainty of input data for room acoustic simulations," in *Proc. of bi-annual Baltic-Nordic Acoustic Meeting*, 2016.

[5] T. Thydal, F. Pind, C.-H. Jeong, and A. P. Engsig-Karup, "Experimental validation and uncertainty quantification in wave-based computational room acoustics," *Appl. Acoust.*, vol. 178, p. 107939, 2021.

[6] C.-H. Jeong, "Design, simulation, and virtual prototyping of room acoustics: Challenges and opportunities," in *International Congress on Acoustics*, 2022.

[7] P. D'Antonio, M. Nolan, E. Fernandez-Grande, and C.-H. Jeong, *Design of a new testing chamber to determine the absorption, diffusion and scattering coefficients*. Universitätsbibliothek der RWTH Aachen, 2019.

[8] ISO 354:2003, "Acoustics — Measurement of sound absorption in a reverberation room," tech. rep., International Organization for Standardization, Geneva, CH, 2003.

[9] V. Wittstock, "Determination of measurement uncertainties in building acoustics by interlaboratory tests. part 2: Sound absorption measured in reverberation rooms," *Acta Acust United Ac.*, vol. 104, pp. 999–1008, 2018.

[10] A. G. Prinn, A. Walther, and E. A. P. Habets, "Estimation of locally reacting surface impedance at modal frequencies using an eigenvalue approximation technique," *J. Acoust. Soc. Am.*, vol. 150, pp. 2921–2935, 2021.

[11] G. Dutilleux, F. C. Sgard, and U. R. Kristiansen, "Low-frequency assessment of the in situ acoustic absorption of materials in rooms: an inverse problem approach using evolutionary optimization," *Int. J. Numer. Meth. Engng.*, vol. 53, no. 9, pp. 2143–2161, 2002.

[12] R. Anderssohn and S. Marburg, "Nonlinear approach to approximate acoustic boundary admittance in cavities," *J. Comput. Acoust.*, vol. 15, no. 1, pp. 63–79, 2007.

[13] G. P. Nava, Y. Yasuda, Y. Sato, and S. Sakamoto, "On the in situ estimation of surface acoustic impedance in interiors of arbitrary shape by acoustical inverse methods," *Acoust. Sci. & Tech.*, vol. 30, no. 2, pp. 100–109, 2009.

[14] A. Bockman, C. Fackler, and N. Xiang, "Bayesian-based estimation of acoustic surface impedance: Finite difference frequency domain approach," *J. Acoust. Soc. Am.*, vol. 137, no. 4, pp. 1658–1666, 2015.

[15] A. J. Hull and C. J. Radcliffe, "An eigenvalue based acoustic impedance measurement technique," *J. Vib. Acoust.*, vol. 113, no. 2, pp. 250–254, 1991.

[16] T. Nowakowski, N. Bertin, R. Gribonval, J. de Rosny, and L. Daudet, "Membrane shape and boundary conditions estimation using eigenmode decomposition," in *Proc. IEEE International Conference on Acoustics, Speech and Signal Processing (ICASSP), Shanghai, China*, Mar. 2016.

[17] E. Brandão, A. Lenzi, and S. Paul, "A Review of the *In Situ* Impedance and Sound Absorption Measurement Techniques," *Acta Acust. united Ac.*, vol. 101, pp. 443–463, 2015.

[18] A. G. Prinn, C. Tuna, A. Walther, and E. A. P. Habets, "Acoustic eigenvalue estimation using the matrix pencil method and rayleigh quotient iteration," in *Forum Acusticum, Turin, Italy*, Sept. 2023.

[19] Y. Hua and T. K. Sarkar, "Generalized pencil-of-function method for extracting poles of an EM system from its transient response," *IEEE Trans. Antennas Propag.*, vol. 37, no. 2, pp. 229–234, 1989.

[20] R. Mohammadi-Ghazi and O. Büyüköztürk, "Sparse generalized pencil of function and its application to system identification and structural health monitoring," in *Proc. SPIE 9805*, Smart Structures and Materials + Nondestructive Evaluation and Health Monitoring, Las Vegas, Nevada, United States, Mar 2016.

[21] J.-H. Lee and H.-T. Kim, "Natural frequency extraction using generalized pencil-of-function method and transient response reconstruction," *Prog. Electromagn. Res. C.*, vol. 4, pp. 65–84, 2008.

[22] A. G. Prinn, "A finite element study of absorption coefficient measurement at low frequencies," in *Inter-Noise, Chiba, Japan*, Aug. 2023.

[23] C. Geuzaine and J.-F. Remacle, "Gmsh: A 3-D finite element mesh generator with built-in pre- and post-processing facilities," *Int. J. Numer. Meth. Engng.*, vol. 79, no. 11, pp. 1309–1331, 2009.

[24] ISO 10534-2:1998, "Determination of sound absorption coefficient and impedance in impedance tubes — Part 2: Transfer-function method," tech. rep., International Organization for Standardization, Geneva, CH, 1998.

[25] M. Karjalainen, P. Antsalo, A. Mäkivirta, T. Peltonen, and V. Välimäki, "Estimation of modal decay parameters from noisy response measurements," *J. Audio Eng. Soc.*, vol. 50, no. 11, pp. 867–878, 2002.

[26] ISO 10534-1:1996, "Determination of sound absorption coefficient and impedance in impedance tubes — Part 1: Method using standing wave ratio," tech. rep., International Organization for Standardization, Geneva, CH, 1996.